Polymer Chemistry

Accepted Manuscript

ROYAL SOCIETY OF CHEMISTRY

www.rsc.org/polymers

Polymer Chemistry

RSCPublishing

PAPER

Electrospun Glycopolymer Fibers for Lectin Recognition

Cite this: DOI: 10.1039/xoxxoooooox

Lei Wang, [a] Gareth R. Williams, [b] Hua-li Nie, [a] Jing Quan, [*a] and Li-min Zhu [*a]

Received ooth January 2012,
Accepted ooth January 2012

DOI: 10.1039/xoxxoooooox

www.rsc.org/

The thermoresponsive glycopolymers poly- (N-isopropylacrylamide-co-6-O-vinyladipoyl-D-glucose) (poly-NIPAM-co-OVDG; PND) and poly-(N-isopropylacrylamide-co-6-O-vinylazelaicoyl-D-glucose) (poly-NIPAM-co-OVZG; PNZ) have been prepared by free radical polymerization process, and subsequently processed into blended fibers with poly-L-lactide-co-ε-caprolactone (PLCL) using electrospinning. The fibers were found to inhibit non-specific adsorption of bovine serum albumin onto their surfaces, but could selectively recognize the lectin Concanavalin A (Con A). The adsorbed Con A can easily be desorbed with a glucose solution. The synthesized fibers were found to have excellent biocompatibility with HeLa cells using the MTT assay, but when loaded with Con A could be used to induce death in the cell population.

Introduction

Carbohydrates play a major role in many biological processes, often by dint of their interaction with proteins. [1-3] To understand and attempt to manipulate these interactions, a large variety of glycopolymers have been designed and synthesized; a number of recent papers discuss these in detail. [4-9] Glycopolymers can be prepared from a range of highly purified monomers, leading to the ability to precisely design their composition and elucidate structure/property relationships. [10] They offer a platform in which multiple copies of a saccharide can be presented simultaneously to a protein, thus enhancing their binding affinity and specificity as a consequence of polyvalent interactions. This is known as the "glycoside cluster effect". [11-15]

However, bulk glycopolymers often suffer from significant steric hindrance. Twisting of the polymer chains can result in low efficacy in the recognition of proteins. To ameliorate this issue, many researchers have sought to graft glycopolymer chains to other materials. One example of this is the work of Qian Yang et al., who prepared glycopolymer brushes tethered to a polypropylene microporous membrane (PPMM) support. [15] The porous structure offers a large surface area for the attachment of glycopolymer chains, and subsequently high sugar density can be achieved because the tethered polymer "brushes" can stretch away from the bulk material to avoid overlap and interference. This results in enhanced recognition properties. [16]

Polymers based on poly (N-isopropylacrylamide) (PNIPAM) undergo large volume changes between their collapsed and swollen states. [16-20] These can be triggered by temperature changes, and thus PNIPAM systems may be employed to deliver controllable protein uptake and discharge. [21] If glucose moieties were incorporated, these resultant materials could have the potential to overcome the steric hindrance problem described above if the polymer conformation could be controlled. PNIPAM/glucose polymers might thus enhance the efficacy of glucose moieties in biological recognition with specific lectins such as Concanavalin A (Con A). Con A is a lectin which shows high specificity for α-D-mannose, α-D-glucose and, to a lesser extent, β-D-glucose with free 3-, 4-, and 6-hydroxyl groups. [22]

Con A is also a well-known activator of cellular signaling. [23] The formation of macromolecular Con A-ligand assemblies on the cell surface appears to be important for signal transduction. [24-26] Recent studies have revealed that proteins with legume lectin domains (such as Con A) can induce apoptosis in HeLa cells and human liver hepatocellular carcinoma HepG2 cells. [27, 28] As a result, two important applications of PNIPAM/glucose copolymers may be envisaged: first, in the sensing of lectins such as con A, and secondly as programmable delivery systems to induce cell apoptosis of cancerous tissue.

In this work, we first prepared thermoresponsive polymers by the free radical copolymerization method. N-isopropylacrylamide (NIPAM) was copolymerized with 6-O-vinyladipoyl-D-glucose (OVDG) to give poly-NIPAM-co-OVDG, or with 6-O-vinylazelaicoyl-D-glucose (OVZG) to give poly-NIPAM-co-OVZG. These syntheses were undertaken in accordance with a literature protocol. [29] Electrospinning was then used to prepare nanofibrous membranes comprising blends of poly-NIPAM-co-OVDG/poly-NIPAM-co-OVZG and poly-L-lactide-co-ε-caprolactone. The fibers' performance in non-selective and selective protein adsorption was subsequently

assessed, as was their ability to deliver apoptosis-inducing agents to cancer cells.

Experimental

Materials

N-isopropylacrylamide (NIPAM, Tokyo Chemical Industry Co. Ltd., Tokyo, Japan, 98 %) was recrystallized from n-hexane. Poly-L-lactide-co-ε-caprolactone (PLCL) was supplied by the Shandong Province Institute of Medical Equipment (Jining, China). 2-[4-(2-Hydroxyethyl)-1-piperazinyl] ethanesulfonic acid (HEPES) was procured from the Nanjing Robiot Co. (Nanjing, China) and was used as received. 2,2' -azo-bio-iso-butyronitrile (AIBN; Sinopharm Chemical Reagent Co., Ltd, Shanghai, China; 97 %) was purified by recrystallization from a 95 % ethanol solution. Dimethyl sulfoxide (DMSO) was purchased from the China National Medicines Corporation Ltd. (Beijing, China). All chemicals used were dried by storing over activated 4 Å molecular sieves for 24 h prior to use. Bovine serum albumin (BSA, purity > 98%) was purchased from the Sino-American Biotechnology Company (Shanghai, China). Con A was obtained from Sigma-Aldrich (Shanghai, China). Fluorescently-labeled Con A (FITC-Con A) was purchased from Vector Laboratories (Burlingame, CA, USA). Rhodamine-labeled BSA (RBITC-BSA) was purchased from the Beijing Boisynthesis Biotechnology Co., Ltd (Beijing, China) and reconstituted with distilled H_2O before use. Dulbecco's modified Eagle medium (DMEM), penicillin-streptomycin solution and Trypsin-EDTA solution were obtained from Gibco (Tulsa, OK, USA). Water was distilled before use.

Copolymerization

6-O-vinyladipoyl D-glucose (OVDG) and 6-O-vinylazelaicoyl (OVZG) were synthesized using analogous protocols to that reported in previous work. [29] Poly-NIPAM-co-OVDG (PND) and poly-NIPAM-co-OVZG (PNZ) were subsequently synthesized via free radical copolymerization with azodiisobutyronitrile (AIBN) as an initiator. OVDG (0.167 g) or OVZG (0.188 g) and NIPAM (0.5658 g) were mixed and dissolved in anhydrous ethanol (5 mL) in a sealed flask, and AIBN (0.01466 g with PND and 0.02639 with PNZ) added. The mixture was stirred under a nitrogen atmosphere at 60 °C for 8 h. The resultant product was repeatedly dialysed in distilled water using dialysis tubes with a molecular weight cut-off of 3500 Dalton, and then dried under vacuum to yield a white copolymer. A total of six copolymers were prepared: PND-1, PND-2, and PND-3, with OVDG: NIPAM ratios of 1:5, 1:10, and 1:15 respectively, and PNZ-1, PNZ-2 and PNZ-3 with OVZG : NIPAM ratios of 1:7, 1:15, and 1:20 respectively. To facilitate comparisons, PNIPAM was also prepared using analogous procedures but without OVDG or OVZG present in the reaction mixture.

Electrospinning

PND and PNZ adsorb water very readily: hence, in order to reduce the hygroscopicity of the fibers resulting from electrospinning blends of PND/PNZ and PLCL were employed. PND/PNZ and PLCL were dissolved in a mixture of dichloromethane and acetone (2:1 v/v) at ambient temperature under gentle stirring for 12 h, forming a homogeneous solution. The total polymer concentration in each solution was 20 wt%. Two different nanofiber compositions were prepared with each PND, one containing PND and PLCL in the ratio 1:1, and the second with ratio 1:2. The PNZ materials had a 1:1 ratio of PNZ : PLCL. Plain PLCL and PNIPAM solutions were also prepared with polymer concentrations of 20 wt%. Full details of the fibers prepared are given in Table 1.

Electrospinning was carried out under ambient conditions (T = 25 ± 3 °C, and relative humidity 65 ± 3 %). The spinning solutions were loaded in a 5 mL syringe fitted with a stainless steel capillary needle (internal diameter 0.5 mm). An electrical potential of 12 kV was applied across a fixed distance (15 cm) between the syringe tip and a collector plate coated in Al foil. This potential was provided using a high voltage power supply (ZGF-2000, Shanghai Sute Electrical Co. Ltd., Shanghai, China). The feed rate of solutions was maintained at 1 mL/h using a single syringe pump (KDS-200, Cole-Parmer®, IL, USA). The resultant fibers were dried for 24 h at 37 °C under vacuum (320 Pa) in a DZF-6050 Electric Vacuum Drying Oven (Shanghai Laboratory Instrument Work Co. Ltd., Shanghai, China) to remove any residual organic solvent and moisture. These setting were used to prepare PND/PLCL and PNZ/PLCL blend fibers, and also plain PLCL and PNIPAM fibers for comparative studies.

Characterization

^{1}H NMR spectra were recorded with TMS as an internal standard using a Bruker DRX 400 MHz spectrometer (Bruker, Rheinstetten, Germany).

The morphology and the diameter of the electrospun nanofibers were analyzed with scanning electron microscopy (SEM; JSM-5600 LV microscope, JEOL, Tokyo, Japan) after the samples were coated with a 20 nm gold layer. The average fiber diameter for each sample was calculated by measuring around 100 fibers in SEM images using the Image J software (National Institutes of Health, MD, USA).

Fourier transform infrared spectroscopy (FT-IR) was conducted using a Nicolet-Nexus 670 FT-IR spectrometer (Nicolet Instrument Corporation, WI, USA) over the range 500-4000 cm^{-1}, and with a resolution of 2 cm^{-1}.

Lower critical solution temperature measurement

PND-1, PND-2, PND-3, PNZ-1, PNZ-2, and PNZ-3 were separately dissolved into deionised water, with concentrations between 0.3 and 1.0 g/L. The solution was monitored as a function of temperature at 500 nm using a Lambda 35 UV-spectrophotometer (PerkinElmer Co., Boston, MA, USA) fitted with a TB-85 Thermo Bath attachment (Shimadzu, Kyoto, Japan) thermostat. The mixed solutions were heated from 23 °C to 45 °C at a heating rate of 0.5 °C/min.

Water contact angle measurement

A contact angle system (322 W, Thermo Cahn Co., WI, USA) was used for the measurement of water contact angles at room temperature in air. Static contact angles were measured with the sessile drop method. A 2 μL drop of water was placed onto the dry surface of a fiber mat with a microsyringe and measurements recorded at least 10 times; results are reported as mean ± S.D.

Confocal microscopy

FITC-Con A (labeled with fluorescein isothiocyanate) was used as a fluorescent probe to evaluate the interactions between Con A and the PND/PNZ-containing fibers. RBITC-BSA (Rhodamine B isothiocyanate-labeled BSA) was used to study non-selective adsorption. A 0.05 ± 0.009 mg sample of each fiber mats was obtained by spinning for a short time directly onto a glass slide, and then used for measurement. 200 μL of FITC-Con A (0.1 mg/mL) or a mixed FITC-Con A and RBITC-BSA mixed solution (0.1 mg/mL with respect to each protein) in HEPES buffer solution (pH 7.5, 10×10^{-3} M HEPES supplemented with 0.1 mM Ca^{2+}, 0.01 mM Mn^{2+} and 0.15 mM Na^{+}) was placed upon the fiber mat. The samples were then incubated at 37 °C for 2 h. [30] After this time, the fiber samples were recovered and washed with HEPES buffer solution eight times to remove any free proteins, before being dried under vacuum at 30 °C for 8 h. Confocal laser scanning microscopy (CLSM; Carl Zeiss LSM700, Jena, Germany) was employed to analyse the fiber mats after immersion.

Temperature influence on protein adsorption

Experiments were performed to elucidate the influence of temperature on protein adsorption. 200 μL of the FITC-Con A solution (0.1 mg/mL in HEPES buffer solution as detailed above) was added to the wells of a 24-well plate and ca. 0.05 mg of each fiber sample added. The resultant mixtures were incubated at 25 °C or 37 °C for 2 h. After this time, the fiber samples were recovered and washed with HEPES buffer solution eight times to remove any free FITC-Con A, before being dried under vacuum at 30 °C for 8 h. Confocal laser scanning microscopy was employed to analyse the fiber mats after immersion.

Elution of adsorbed proteins

These fiber mats which had been treated with FITC-Con A or RBITC-BSA were placed into 200 μL of a 1 M glucose solution in a HEPES buffer (pH 7.5, containing 10 mM HEPES, 0.15 M NaCl, 0.1 mM Ca^{2+}, 0.01 mM Mn^{2+}, 0.08% sodium) and incubated at 25 °C or 37 °C (the same temperature was used for elution as for adsorption) for 24 h. The solid fiber mat and the eluent were separated and the fiber mats washed with HEPES buffer solution 6 times. HEPES buffer was used to dilute the eluent to a volume of 5 mL, and a fluorescence spectrophotometer (F-4500, Hitachi, Tokyo, Japan) employed to investigate the solution. The fiber mats were analysed by CLSM as detailed above.

Interaction with HeLa cells

Cell culture.
HeLa cervical cancer cells were obtained from the Chinese Academy of Sciences Type Culture Collection. Cells were maintained as an exponentially growing monolayer in a DMEM high sugar medium supplemented with 10 % fetal bovine serum, and 1 % (v/v) penicillin/streptomycin solution (Gibco, Germany). The cells were cultured at 37 °C in a humidified atmosphere containing 5 % CO_2. Cells were passaged every 1-2 days. For passaging, the cells were trypsinized with 0.5/0.2 % (v/v) trypsin/EDTA solution (Gibco).
MTT assays.
The cytotoxic effects of the fibers on HeLa cells were measured with the MTT assay. 400 μL of logarithmically growing HeLa cells (5×10^5 cells/mL) were seeded into 24-well plates. A glass slide with ca. 0.05±0.009 mg fibers on it was added to each well, and the plates cultured for 48 h in an incubator (37 °C, 5% CO_2). The supernatant was then removed and the cells washed with phosphate buffered saline (PBS, pH = 7.36, ionic strength 10 mM). 360 μL of a DMEM high sugar medium without bovine serum or penicillin/streptomycin and 40 μL of a MTT solution (5 μg/mL) were placed into each well and the cells incubated for a further 4 h in the dark. After discarding the supernatant, the foramen grains formed by viable cells were solubilized with DMSO (400 μL/well) and shaken for 30 min at room temperature in the dark. The optical density (OD) was finally measured at 570 nm with a Microplate Reader (Thermo Multiskan MK3, Thermo Scientific Company, Waltham, Britain). Experiments were also performed to assess viability after culture with the fibers for four and six days. Cell viability was calculated as:

$$\text{viable rate (\%)} = \frac{\text{OD}_{\text{treated}}}{\text{OD}_{\text{control}}} \times 100$$

where $OD_{control}$ is that observed with cells cultured in the absence of fibers and $OD_{treated}$ that obtained in the presence of fibers. The optical density is in direct proportion to cell viability.

Further experiments were performed in which 400 μL of a 0.72 mg/mL Con A solution in HEPES buffer (pH 8.5, containing 10 mM HEPES, 0.1 mM Ca^{2+}, 0.008% sodium azide) was initially incubated with the PND fiber mats for 4 hours. The Con A solution was then removed, and the fibers washed eight times with HEPES buffer before being added to cell culture, and treated as detailed above.

Results and discussion

Characterization of PND and PNZ

The synthesis of PND/PNZ-type polymers has been reported previously. [29] These literature procedures were followed here, and the success of the experiments determined through NMR and IR spectroscopies. The FT-IR spectra for PNIPAM, Poly-OVDG, PND, Poly-OVZG, and PNZ are depicted in Figure S1. The spectrum of PNIPAM (Figure S1(A)) shows important bands at ca. 1644 cm^{-1} (-C=O), and 3295 cm^{-1} (-NH-). The Poly-OVDG (Figure S1(B)) shows characteristic peaks at 2932 cm^{-1} (C-H stretching), 2914 cm^{-1} (-CH_2-stretching), and 1742 cm^{-1} (O-C=O of carboxylic acid). The spectrum of PND (Figure S1(C)) demonstrates differences in the vibrational modes corresponding to both its PNIPAM and Poly-OVDG components demonstrating successful polymerization. The Poly-OVZG (Figure S1 (D)) shows characteristic peaks at 2930 cm^{-1} (C-H stretching), 2857 cm^{-1} (-CH_2-stretching), 1733 cm^{-1} (O-C=O of carboxylic acid), 3391 cm^{-1} (-OH on the glucose). The spectrum of PNZ (Figure S1 (E)) also demonstrates differences in the vibrational modes corresponding to both its PNIPAM and Poly-OVZG components demonstrating successful polymerization.

Successful polymerization is also evidenced from ^{1}H NMR spectra. ^{1}H NMR data for Poly-OVDG and PND are given in Figure S2. The ^{1}H NMR spectrum of PNIPAM and the Poly-OVDG indicate successful polymerization. The full ^{1}H NMR data of PND may be assigned as follows: ^{1}H NMR (400 MHz; D_2O, Me_4Si) δ 7.79 (1-H of-NH-), 5.09-2.58 (CHO; 1-H, 2-H, 3-H, 4-H, 5-H, 6-H, 1′-H, 2′-H, 3′-H, 4′-H ,5′-H, and 6′-H of -D-glucose and β-D-glucose), 2.34-2.26 (m, 2H, 2-$COCH_2CH_2$-),

2.09-1.95 (m, 3H, 2-$COCH_2CH_2$-, -$CH(CH_3)_2$), 1.51-1.02 (m, 16 H, -$CH(CH_3)_2$). ^{1}H NMR data for OVZG and PNZ are given in Figure S3: The full ^{1}H NMR data of PNZ may be assigned as follows: ^{1}H NMR (400 MHz; D_2O, Me_4Si) δ 5.08-3.12 (CHO; 1-H, 2-H, 3-H, 4-H, 5-H, 6-H, 1′-H, 2′-H, 3′-H, 4′-H ,5′-H, and 6′-H of -D-glucose and β-D-glucose), 3.67 (m, 1H, -$CH(CH_3)_2$), 2.31-1.83 (m, 4H, -CO-CH_2-$(CH_2)_5$-CH_2-CO-), 1.45-1.20 (m, 10H, -CO-CH_2-$(CH_2)_5$-CH_2-CO-), 1.02 (d, 6H, -$CH(CH_3)_2$). Details of all of glycopolymers are shown in Table 1.

Table 1

Lower critical solution temperature (LCST)

The LCST of the polymer solutions was determined by monitoring the change in optical absorbance at 500 nm on heating: the data are given in Figures 1 and 2. The phase transition temperature becomes higher as the OVDG and OVZG contents increase, in agreement with literature reports showing that the LCST of NIPAM co-polymers rises with an increasing content of hydrophilic monomers. [31, 32] The LCST transitions are observed to be very sharp, occurring over a narrow temperature range (ca. 3 °C). The LCSTs of PND-1 (highest OVDG content), PND-2 and PND-3 (lowest OVDG content) are 39 °C, 36 °C and 34 °C, as compared to 32 °C for the pure PNIPAM homopolymer. The analogous values for PNZ-1 (highest OVZG content), PNZ-2 and PNZ-3 (lowest OVZG content) are 36 °C, 35 °C and 34 °C. This increase in LCST with increasing glucose monomer content is expected to arise because as the OVDG and OVZG content increases, there are increasing numbers of hydrogen bonds which can form between solution water molecules and glucose hydroxyl groups. Hence more energy and a higher temperature are required to expel the water from the polymer matrix and effect the coil to globule transition.

Figure 1.

Figure 2.

Electrospun nanofibers

In electrospinning, there are several key processing parameters including solution concentration, electrical field strength, and feed rate that have profound effects on the properties of the fibers produced. [33] For the spinning of PND/PLCL and PNZ/PLCL blends, the optimized conditions were found to be a solution containing 20 wt % of total polymer (PND/PLCL or PNZ/PLCL respectively), a feed rate of 1.0 mL/h, and an electric field strength of 12.0 kV, with a distance of 15 cm between spinneret and collector. The compositions of the various fibers produced are listed in Table 2. SEM images of the different PND/PLCL and PNZ/PLCL fibers are shown in Figure 3. The fibers can all be observed to be cylindrical in shape, with smooth surfaces and no obvious “bead on string” morphology. The average diameters of the fibers, as determined using the Image J software, are detailed in Table 2. The fibers containing PND-1 and the PNIPAM/PLCL fibers are found to be much wider than the rest of the materials, with diameters of one micron or more. The reason behind this is not certain, but it may be that because the fibers containing PND-1 own the highest OVDG content, they have the greatest hydrophilicity and hence may retain more of the solvent used for electrospinning than the other materials. The fibers of PND-2 and PND-3 are much smaller in size, and the PND:PLCL ratio appears to have little influence on fiber size. Fibers incorporating PNZ-1, PNZ-2, and PNZ-3 are all also approximately the same size in diameter, and again changing the PNZ:PLCL ratio in the polymer blend has little effect on the size.

Figure 3.

Table 2.

Water contact angle measurements

The hydrophilicity of the PND/PLCL, PNZ/PLCL and PLCL fibers were evaluated by water contact angle measurements. The results are shown in Figure 4, and indicate that as the OVDG (Figure 4 (A)) and OVZG (Figure 4 (B)) content in the polymers used for fiber formation increases, the water contact angle is generally reduced. A dramatic decline in contact angle is seen from 112. 6º (PLCL) to 28. 6º (for polymers with a PND: PLCL ratio 1:1) or 30. 4º (PND: PLCL ratio 1: 2), and to 29.8o (PNZ/PLCL fibers) as the glucose monomer : NIPAM ratio rises from 0 to 1:5 (PND) or 1:10 (PNZ). The results revealed that the glycosylated membrane ssurfaces are extraordinarily hydrophilic, with increasing hydrophilicity correlated to increased glucose monomer content. The surface hydrophilicity of the PND and PNZ fibers will play an important role in their performance as biomaterials. [34]

Figure 4.

Confocal microscopy studies

A series of adsorption and desorption experiments at 37 °C were undertaken to explore whether the PND-containing fibers were able to selectively absorb lectins. Fiber mats were incubated with a mixture of FITC-Con A and RBITC-BSA, and high-resolution confocal microscopy images are given in Figure 5. Calibration curves for the two fluorescent proteins (FITC-Con A and RBITC-BSA) are shown in the Supplementary Information Figure S4.

Figure 5.

It can be seen that the FITC fluorescence intensity of the PND-containing fibers is much stronger than that of PLCL or PLCL/PNIPAM fibers. This suggests that the PND-containing fibers can adsorb Con A where the control samples cannot. This can be ascribed to the fact that PLCL and PNIPAM lack any glucose groups which can interact specifically with Con A. None of the fibers appear to absorb much BSA, given the very low levels of RBITC fluorescence seen in Figure 5 (A). The fibers can discharge their protein loads effectively when immersed in a glucose solution (Figure 5 (B)).

Quantitative measurement of the protein uptake as measured by a fluorescence spectro-photometer showed very clearly (Figure 6) that the PND-containing fibers are highly selective for Con A. The glucosylated fibers described here can thus participate in selective protein recognition and adsorption while remaining inert to non-specific adsorption of protein. [35] The data in Figure 6 also clearly show the effective desorption of Con A upon exposure to a glucose solution.

Figure 6.

Identical experiments were performed with the PNZ materials, and the results can be found in Figure 7 and Figure 8. The results are very similar to those for the PND-based fibers, with the PNZ materials showing minimum BSA adsorption, and much enhanced Con A uptake over the PNIPAM/PLCL fibers.

Figure 7.

Figure 8.

The influence of temperature on Con A adsorption was explored for the PND-based materials, and is shown in Figures 9 and 10. Adsorption at 25 °C is clearly greater than at 37 °C,

as demonstrated by the greatly increased FITC fluorescence visible at the former temperature. These experiments were performed over 2 h. Over prolonged periods of time, it appears that the equilibrium absorption is about the same at both 25 and 37 ºC, but the data in Figure 9 suggest that adsorption occurs more rapidly at 25 °C. After desorption, the fluorescence intensity of the fibers reduces almost to nothing, confirming the effective desorption of Con A from the materials.

Figure 9.

Figure 10.

Fiber biocompatibility

The biocompatibility of the PND and PNZ fibers was explored using the MTT assay; results are included in Figure 14. From the data given in Figure 11 (A), it is clear that the fibers have very generally good biocompatibility. The optical density increases continuously with the culture time, indicating a growing cell adhesion and cell viable rate, and when compared to the untreated control group the fiber-treated wells have the same or greater cell populations. The data in Figure 11 (B) show the results of an analogous experiment but with Con A-loaded fiber mats. The adsorption values after 4 or 6 days' culture are much reduced from those with the untreated fibers, demonstrating that under the cell culture conditions, the fibers can release their Con A loading, and once the Con A was freed into solution, it can initiated cell death by autophagic or apoptotic mechanisms. [27,28]

Figure 11.

Conclusions

Nanofibers containing glycopolymers were prepared via free radical polymerization and electrospinning. The fiber mats were found to inhibit the non-specific adsorption of BSA, but to significantly enhance the specific recognition of Con A. There appears to be an effect of temperature in uptake of Con A, indicating that the materials may be useful for temperature-responsive applications. The adsorbed Con A is easily desorbed upon elution with a glucose solution. The fiber mats have good biocompatibility and minimum cytotoxicity. When the fiber mats are loaded with Con A, they are able to promote HeLa cell death.

A wide range of glycosylated polymers can be prepared, and given their temperature sensitive properties have the potential to generate the sensitive and specific identification of tumor cells scaffolds, drug release carriers and clinical diagnosis.

Acknowledgements

This investigation was supported by the National Natural Science Foundation of China (No.21303014); the UK-China Joint Laboratory for Therapeutic Textiles, the State Key Laboratory for the Modification of Chemical Fibers and Polymer Materials, Key Laboratory of Science & Technology of Eco-Textiles, Donghua University, Ministry of Education, and the Fundamental Reaserch Funds for the Central Universities (Donghua University).

Notes and references

[a] College of Chemistry, Chemical Engineering and Biotechnology, Donghua University, Shanghai, 201620, P.R.China.
[b] UCL School of Pharmacy, 29-39 Brunswick Square, London, WC1N 1AX, UK.

1 S. Cecioni, D. Goyard, J.-P. Praly and S. Vidal, *Methods in molecular biology (Clifton, N.J.)*, 2012, **808**, 57-68.
2 E. Gorelik, U. Galili and A. Raz, *Cancer and Metastasis Reviews*, 2001, **20**, 245-277.
3 V. Ladmiral, E. Melia and D. M. Haddleton, *European Polymer Journal*, 2004, **40**, 431-449.
4 C. Qi, X. Yonghua, D. Yuguo and H. Bao-Hang, *Polymer*, 2009, **50**, 2830-2835.
5 M. Toyoshima and Y. Miura, *Journal of Polymer Science Part a-Polymer Chemistry*, 2009, **47**, 1412-1421.
6 M. Al-Bagoury, K. Buchholz and E.-J. Yaacoub, *Polymers for Advanced Technologies*, 2007, **18**, 313-322.
7 J. Geng, J. Lindqvist, G. Mantovani, G. Chen, C. T. Sayers, G. J. Clarkson and D. M. Haddleton, *Qsar & Combinatorial Science*, 2007, **26**, 1220-1228.
8 G. Gody, P. Boullanger, C. Ladaviere, M.-T. Charreyre and T. Delair, *Macromolecular Rapid Communications*, 2008, **29**, 511-519.
9 M. Toyoshima, T. Oura, T. Fukuda, E. Matsumoto and Y. Miura, *Polymer Journal*, 2010, **42**, 172-178.
10 Haiting Shi, Li Liu,* Xiaobei Wang and Jingyi Li, Polymer Chemistry, 2012, 3, 1182-1188.
11 R. Roy, *Trends in Glycoscience and Glycotechnology*, 2003, **15**, 291-310.
12 Y. M. Chabre and R. Roy, in *Advances in Carbohydrate Chemistry and Biochemistry, Vol 63*, ed. D. Horton, 2010, vol. 63, pp. 165-393.
13 K. Matsuoka, H. Yamaguchi, T. Koyama, K. Hatano and D. Terunuma, *Tetrahedron Letters*, 2010, **51**, 2529-2532.
14 M. Obata, T. Kobori, S. Hirohara and M. Tanihara, *Polymer*, 2012, **53**, 4672-4677.
15 Q. Yang, M.-X. Hu, Z.-W. Dai, J. Tian and Z.-K. Xu, *Langmuir*, 2006, **22**, 9345-9349.
16 G. Li, L. Shi, Y. An, W. Zhang and R. Ma, *Polymer*, 2006, **47**, 4581-4587.
17 B. Trzebicka, B. Robak, R. Trzcinska, D. Szweda, P. Suder, J. Silberring and A. Dworak, *European Polymer Journal*, 2013, **49**, 499-509.
18 N. do Nascimento Marques, P. Schroeder Curti, A. M. da Silva Maia and R. Balaban, *Journal of Applied Polymer Science*, 2013, **129**, 334-345.
19 Z. Liu, Q. Liao, D. Yang, Y. Gao, X. Luo, Z. Lei and H. Li, *Designed Monomers and Polymers*, 2013, **16**, 465-474.
20 C. Wu, A. Ying, S. Ren and J. Xu, *Asian Journal of Chemistry*, 2013, **25**, 3806-3810.
21 T. Trongsatitkul and B. M. Budhlall, *Colloids and Surfaces B-Biointerfaces*, 2013, **103**, 244-252.
22 I. J. Goldstein, C. E. Hollerman and E. E. Smith, *Biochemistry*, 1965, **4**, 876-883.
23 Z. Shi, N. An, S. Zhao, X. Li, J. K. Bao and B. S. Yue, *Cell Proliferation*, 2013, **46**, 86-96.
24 S. Yan, L. Wang, N. Liu, Y. Wang and Y. Chu, *Immunology and Cell Biology*, 2012, **90**, 421-428.
25 T. Nagata, L. McKinley, J. J. Peschon, J. F. Alcorn, S. J. Aujla and J. K. Kolls, *Journal of Immunology*, 2008, **181**, 7473-7479.
26 V. Volarevic, M. Mitrovic, M. Milovanovic, I. Zelen, I. Nikolic, S. Mitrovic, N. Pejnovic, N. Arsenijevic and M. L. Lukic, *Journal of Hepatology*, 2012, **56**, 26-33.
27 C.-P. Chang, M.-C. Yang, H.-S. Liu, Y.-S. Lin and H.-Y. Lei, *Hepatology*, 2007, **45**, 286-296.

28 C.-Y. Li, H.-L. Xu, B. Liu and J.-K. Bao, *Current molecular pharmacology*, 2010, **3**, 123-128.
29 S.-F. Lou, H. Zhang, G. R. Williams, C. Branford-White, H.-L. Nie, J. Quan and L.-M. Zhu, *Colloids and Surfaces B-Biointerfaces*, 2013, **105**, 180-186.
30 Meng-Xin Hu, Ling-Shu Wan, Zhi-Sheng Fu, Zhi-Qiang Fan and Zhi-Kang Xu*, Macromol. Rapid Commun., 2007, 28, 2325-2331.
31 M. E. Alf, T. A. Hatton and K. K. Gleason, *Polymer*, 2011, **52**, 4429-4434.
32 E. S. Gil and S. M. Hudson, *Progress in Polymer Science*, 2004, **29**, 1173-1222.
33 A.-F. Che, X.-J. Huang, Z.-G. Wang and Z.-K. Xu, *Australian Journal of Chemistry*, 2008, **61**, 446-454.
34 H. Zhang, S. Li, C. J. B. White, X. Ning, H. Nie and L. Zhu, *Electrochimica Acta*, 2009, **54**, 5739-5745.
35 B. T. Houseman and M. Mrksich, *Chemistry & Biology*, 2002, **9**, 443-454.

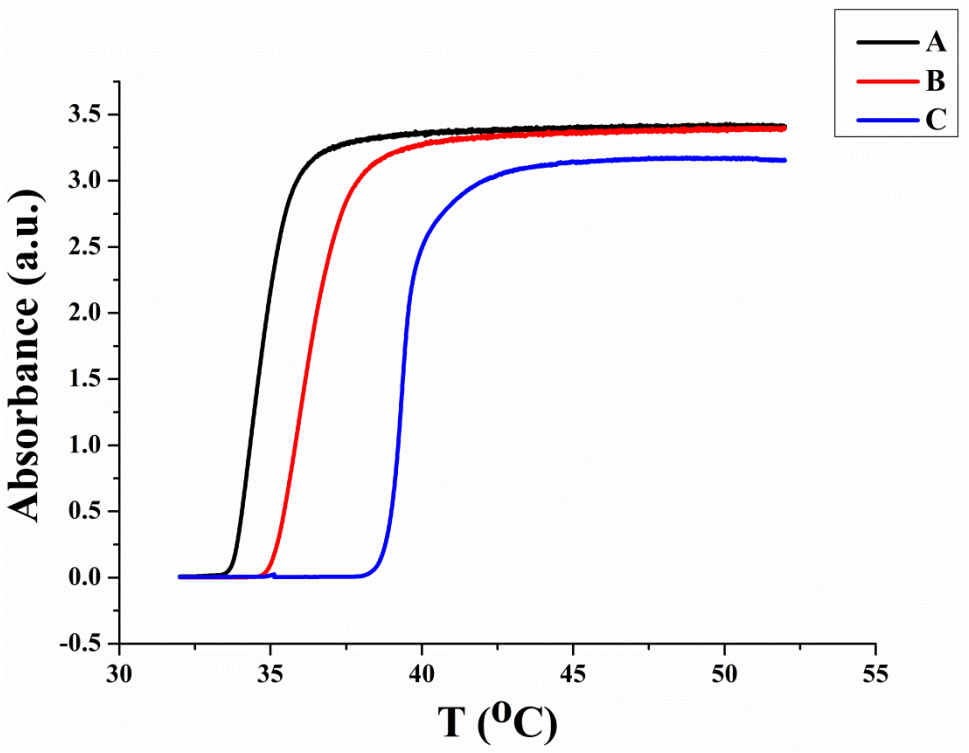

Figure 1. Plot of absorbance vs. temperature for (A) PND-3 (1:15 OVDG : NIPAM); (B) PND-2 (1:10 OVDG : NIPAM); and (C) PND-1 (1:5 OVDG : NIPAM) recorded for 3 mg/mL solutions in water. The heating rate was 0.5 ℃/min.

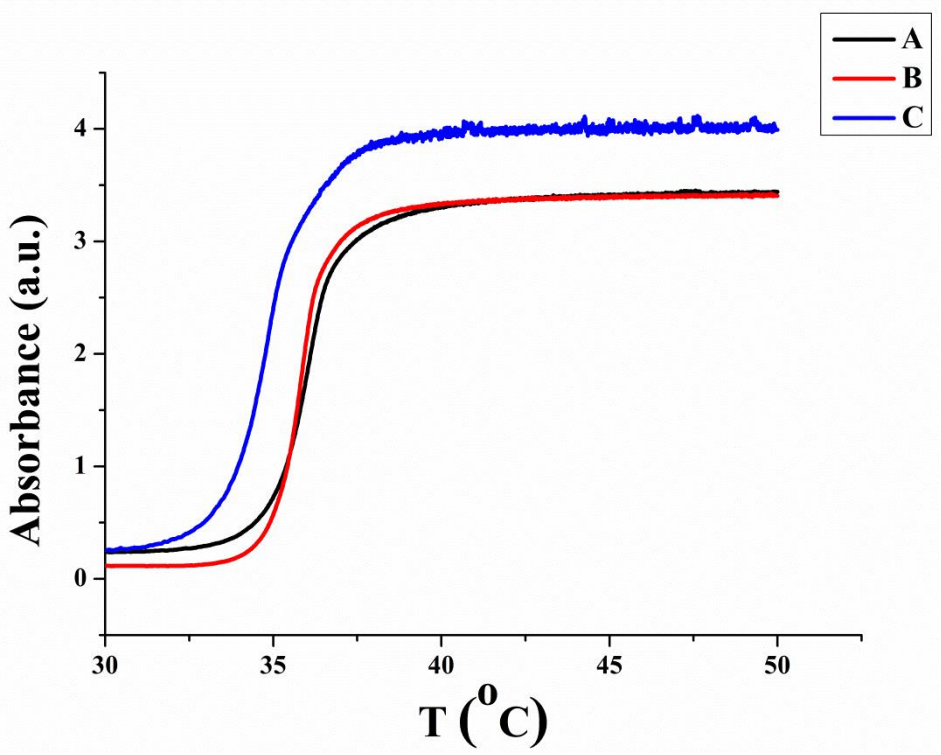

Figure 2. Plot of absorbance vs. temperature for (A) PNZ-1 (1:10 OVZG : NIPAM); (B) PNZ-2 (1:15 OVZG : NIPAM); and (C) PNZ-3 (1:20 OVZG : NIPAM) recorded for 3 mg/mL solutions in water. The heating rate was 0.5 ℃/min.

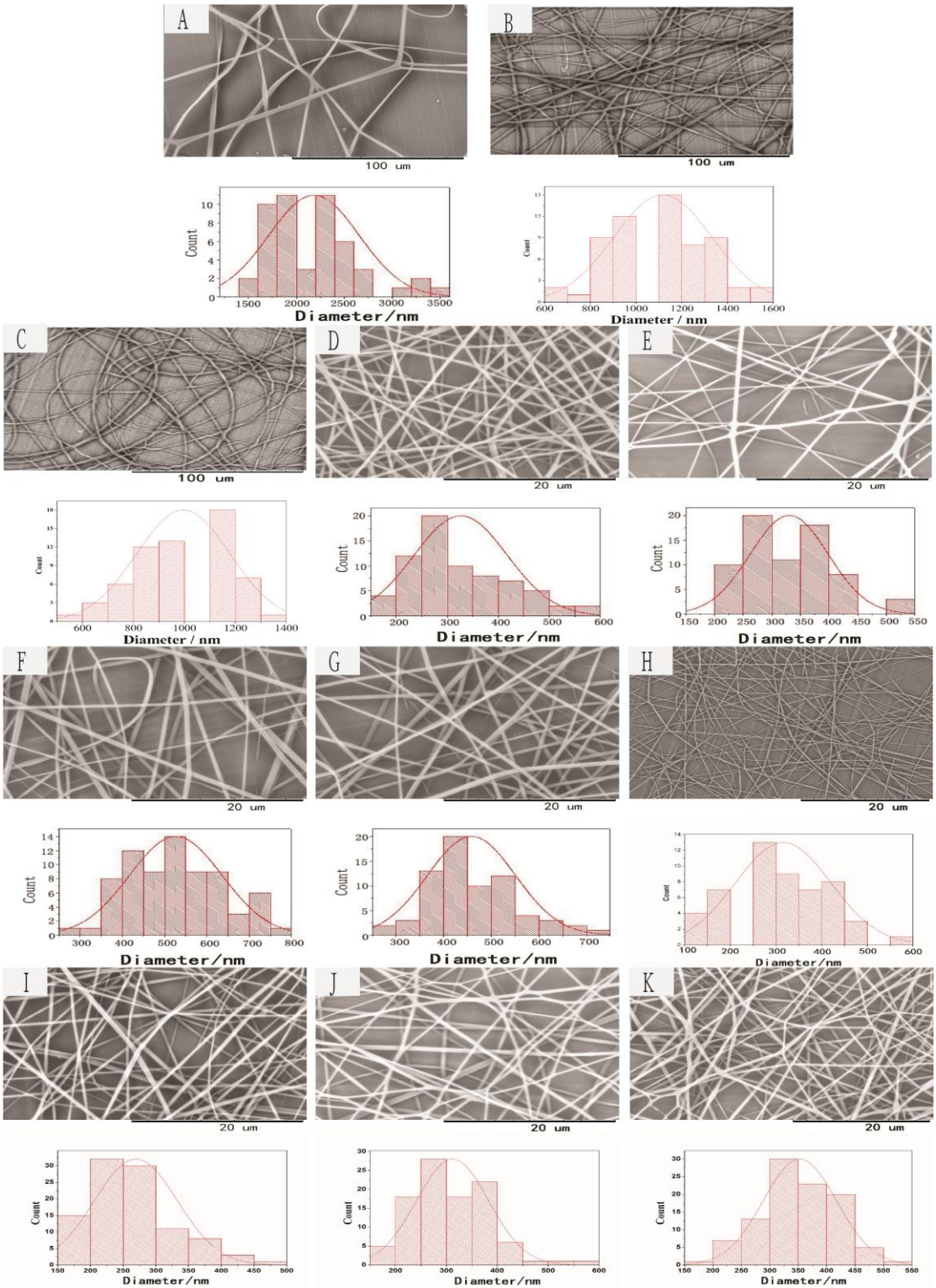

Figure 3. SEM images of the electrospun fibers prepared in this work (A) PNIPAM/PLCL; (B) PND-1-A; (C) PND-1-B; (D) PND-2-A; (E) PND-2-B; (F) PND-3-A; (G) PND-3-B; (H) PLCL; (I) PNZ-1; (J) PNZ-2; (K) PNZ-3.

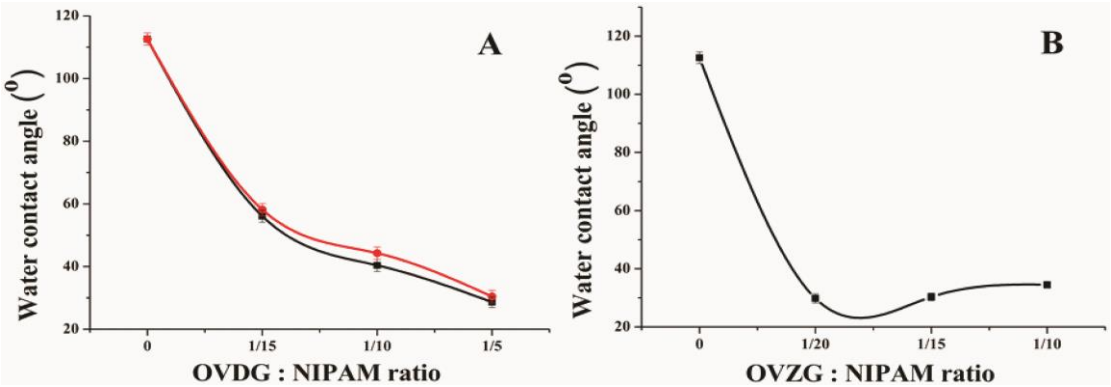

Figure 4. Water contact angle measurements for (A): PND-based and (B): PNZ based fibers. In part (A), the PND-A (1: 1 PND : PLCL ratio) materials are shown in black, and the PND-B samples (1: 2 PND : PLCL) in red.

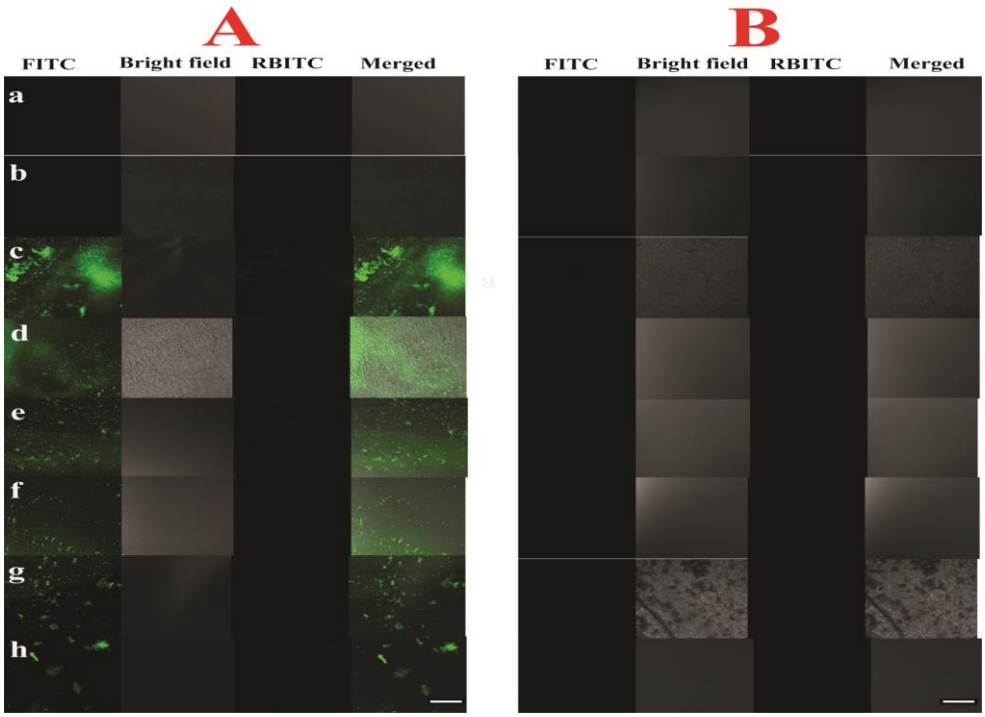

Figure 5. Confocal microscopy images of the PND fibers after interaction with FITC-labelled Con A and RBITC-BSA at 37 ℃: (A) adsorption; (B) desorption; Images are shown for fibers made of (a) PNIPAM/PLCL; (b) PLCL; (c) PND-1-A; (d) PND-1-B; (e) PND-2-A; (f) PND-2-B; (g) PND-3-A; and (h) PND-3-B. The scale bar in each image is 200 μm.

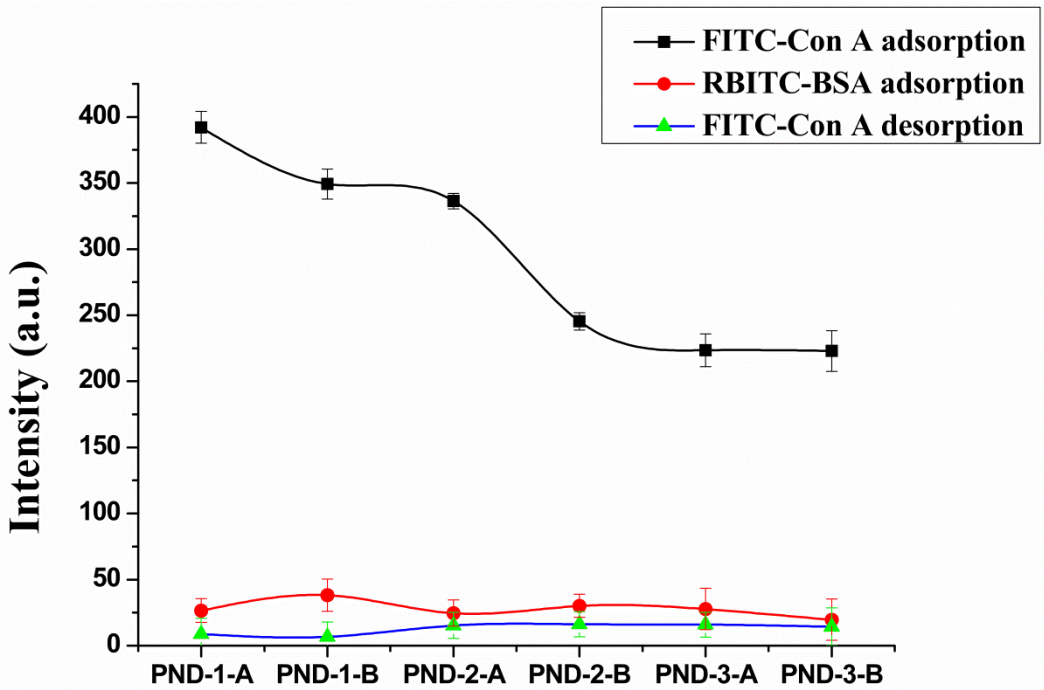

Figure 6. Adsorption and desorption of proteins from the PND fibers as measured using fluorescent spectrophotometry.

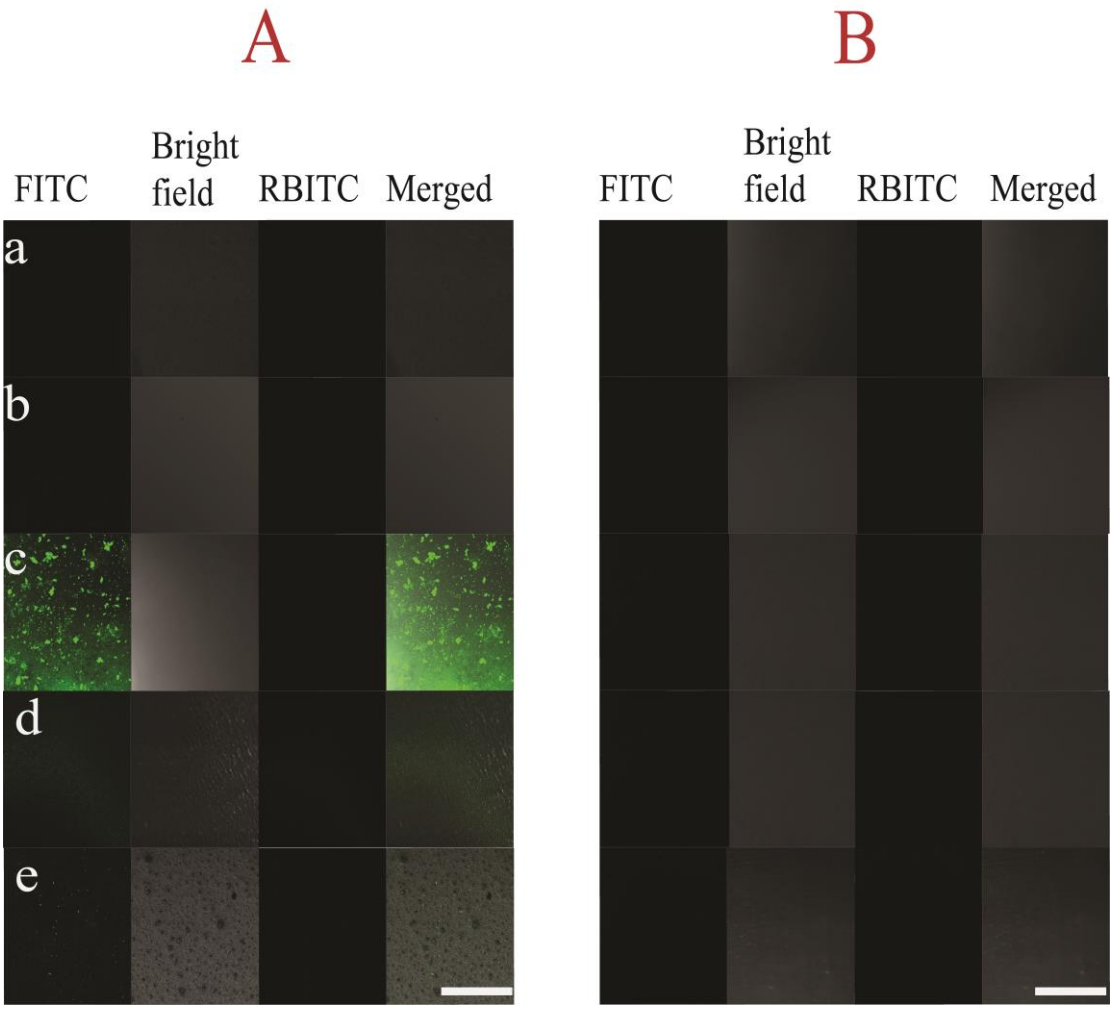

Figure 7. Confocal microscopy images of the PNZ fibers after interaction with FITC-labelled Con A and RBITC-labeled BSA at 37 ℃: (A) adsorption; (B) desorption; Images are shown for (a) PNIPAM/PLCL; (b) PLCL; (c) PNZ-1; (d) PNZ-2; (e) PNZ-3.
The scale bar in each image is 200 μm.

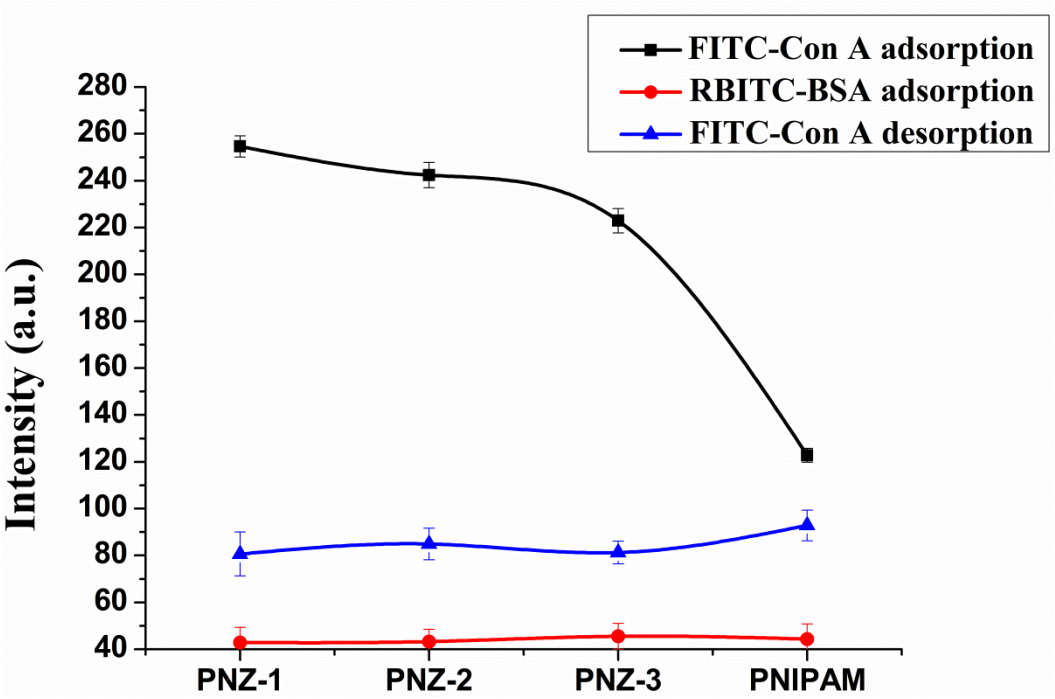

Figure 8. Adsorption and desorption of proteins from the PNZ fibers as measured using fluorescent spectrophotometry.

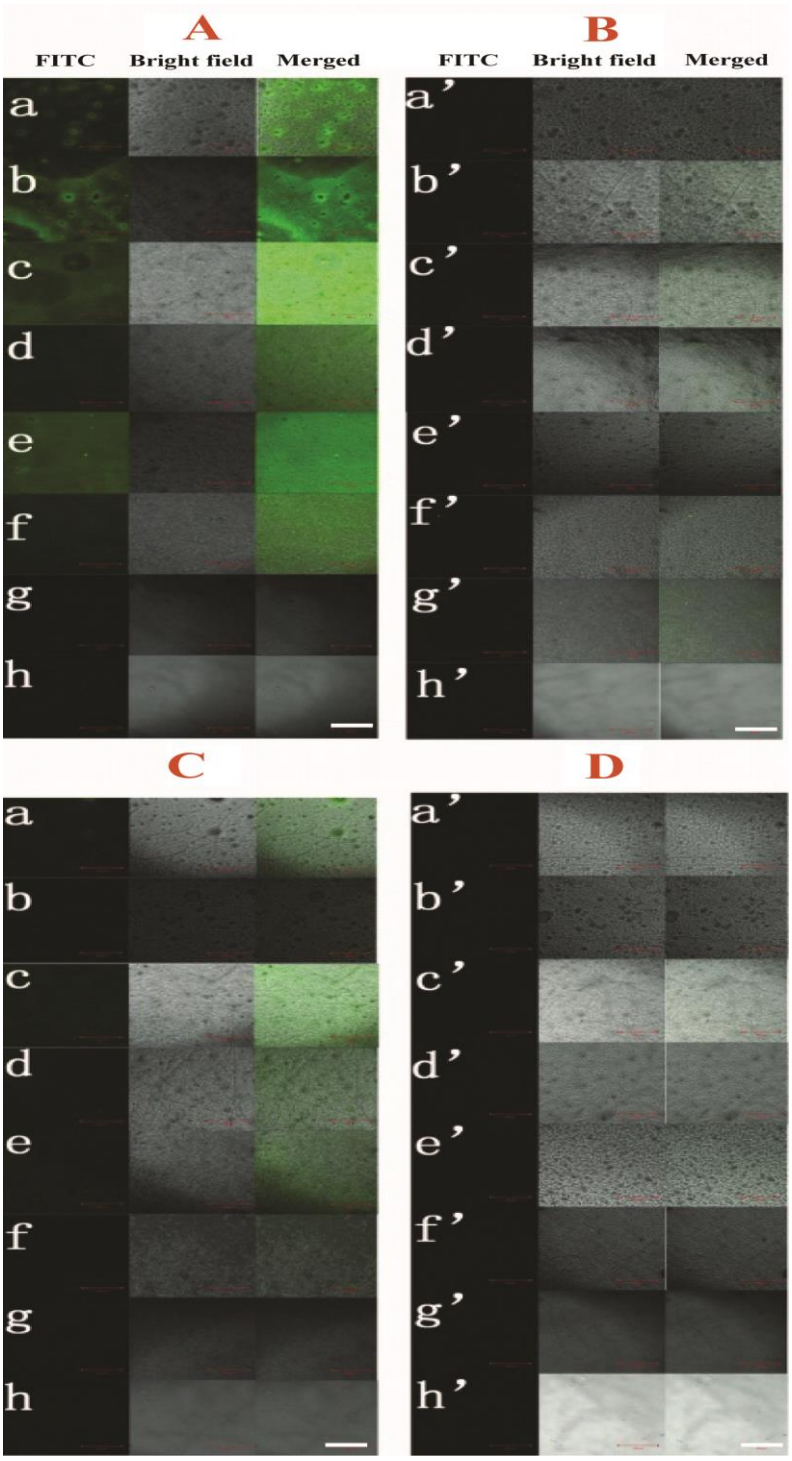

Figure 9. Confocal microscopy images of the PND fibers after interaction with FITC-labelled Con A: (A) adsorption at 25 ℃; (B) desorption at 25 ℃; (C) adsorption at 37 ℃; (D) desorption at 37 ℃ Images are shown for (a) PND-1-A; (b) PND-1-B; (c) PND-2-A; (d) PND-2-B; (e) PND-3-A; (f) PND-3-B; (g) PLCL; and (h) PNIPAM/PLCL.
The scale bar in each image is 200 μm.

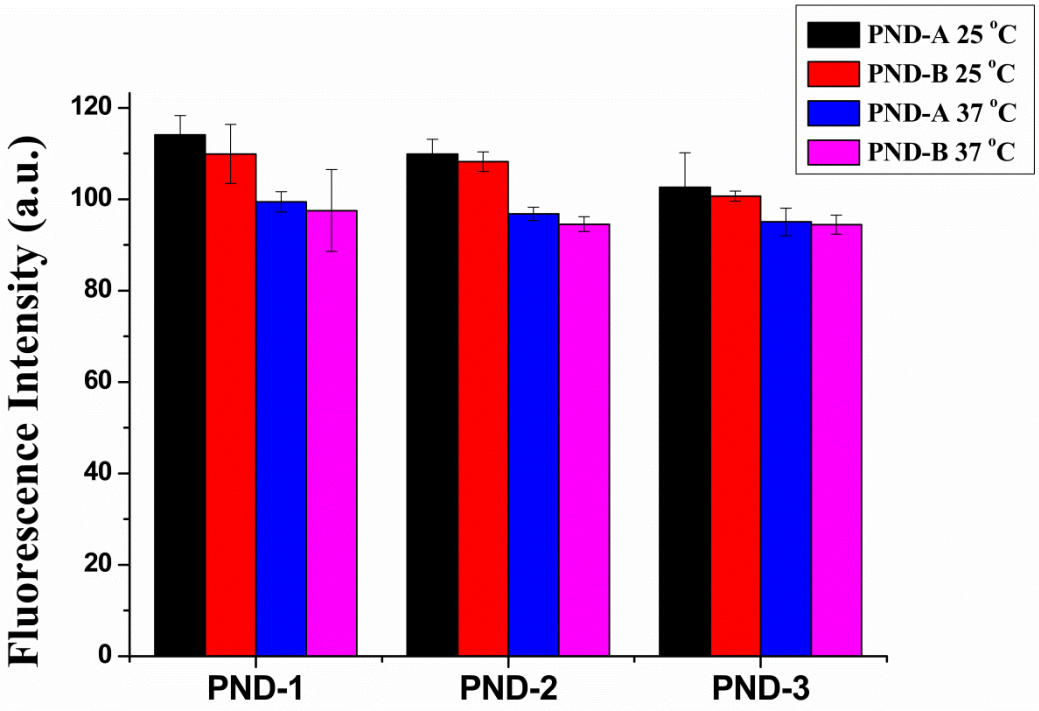

Figure 10. Fluoroscent spectro-photometry measurements of solution fluorescence intensity after desorption of Con A from the fiber mats. PND-A fibers have a 1: 1 ratio of PND : PLCL, and PND-B fibers a 1: 2 ratio.

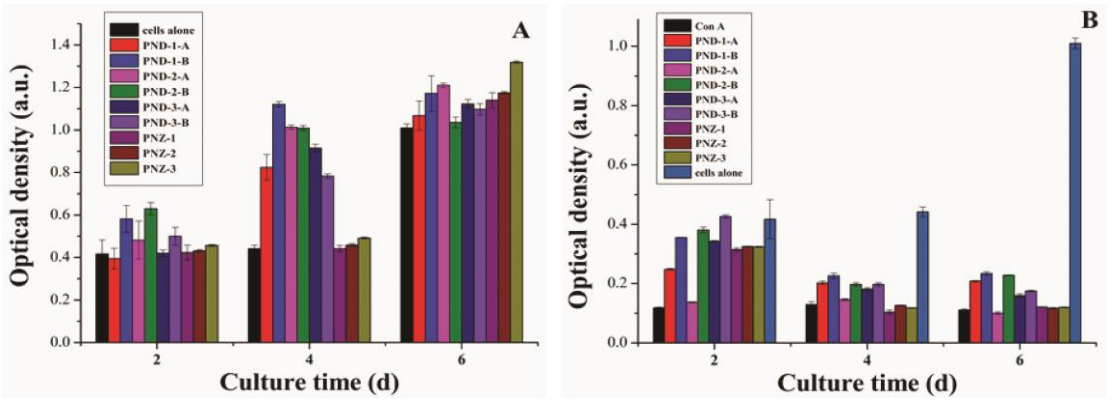

Figure 11. MTT assay results for HeLa cells treated with the PND fibers (A) as-synthesised fibers; (B) Con A-treated fibers. Where Con A in (B) means control group without fibers but treated by Con A.

Table 1

Details of the glycopolymers prepared

Sample ID	Feed Ratio [a]	Weight [b] (g)	Yield [b] (%)	M_n [c] (g/mol)	M_w [c] (g/mol)	PDI [c]	Composition [d]
PND-1	1:5	0.4032	70	68939	104815	1.52	1:5.3
PND-2	1:10	0.5083	68	57331	85423	1.49	1:10.5
PND-3	1:15	0.7493	72	77600	148910	1.92	1:14.6
PNZ-1	1:7	0.5305	68	43242	55745	1.29	1:7.4
PNZ-2	1:15	0.7868	74	58926	71746	1.22	1:15.9
PNZ-3	1:20	1.0499	78	103100	182590	1.77	1:21.01

[a] Feed ratios for PND-1, PND-2, PND-3 are OVDG:NIPAM; feed ratios of PNZ-1, PNZ-2, PNZ-3 are OVZG:NIPAM

[b] Determined by gravimetric analysis

[c] Determined by GPC

[d] PND-1, PND-2, PND-3 ratios refer to OVDG:NIPAM; PNZ-1, PNZ-2, PNZ-3 to OVZG:NIPAM. Determined by ^{1}H NMR measurements in D_2O

Table 2

Characterising data for the electrospun materials (--- indicates that the water disappeared quickly when dropped on the membranes, owing to the very high hydrophilicity of PNIPAM).

Sample ID	Polymer ratio in fibers [a]	Fiber Diameter (nm)	Water Contact Angle (°)	Con A Adsorption [b]	BSA Adsorption [c]
PND-1-A	1:1	1100±200	55.8±5	2.02	0.63
PND-1-B	1:2	1000±200	56.2±5.5	1.80	0.89
PND-2-A	1:1	320±120	40.4±4.2	1.73	0.59
PND-2-B	1:2	330±80	44.3±5.2	1.27	0.71
PND-3-A	1:1	520±120	28.6±5	1.16	0.66
PND-3-B	1:2	470±120	30.4±4.6	1.15	0.47
PNZ-1	1:1	275±75	34.5±4.2	1.32	0.9
PNZ-2	1:1	300±50	30.3±5.1	1.25	1.0
PNZ-3	1:1	350±75	29.8±3.8	1.15	1.0
PLCL	0	300±80	112.6±4.9	___	___
PNIPAM	1:1*	2200±400	---	0.06	1.0

* PNIPAM: PLCL ratio

[a] PND : PLCL or PNZ : PLCL ratios in fibers

[b] Con A adsorption on the fibers calculated using the calibration curve in Figure S4 in mg Con A/mg fiber mat

[c] BSA adsorption on the fibers calculated using the calibration curve in Figure S4 in mg BSA/mg fiber mat

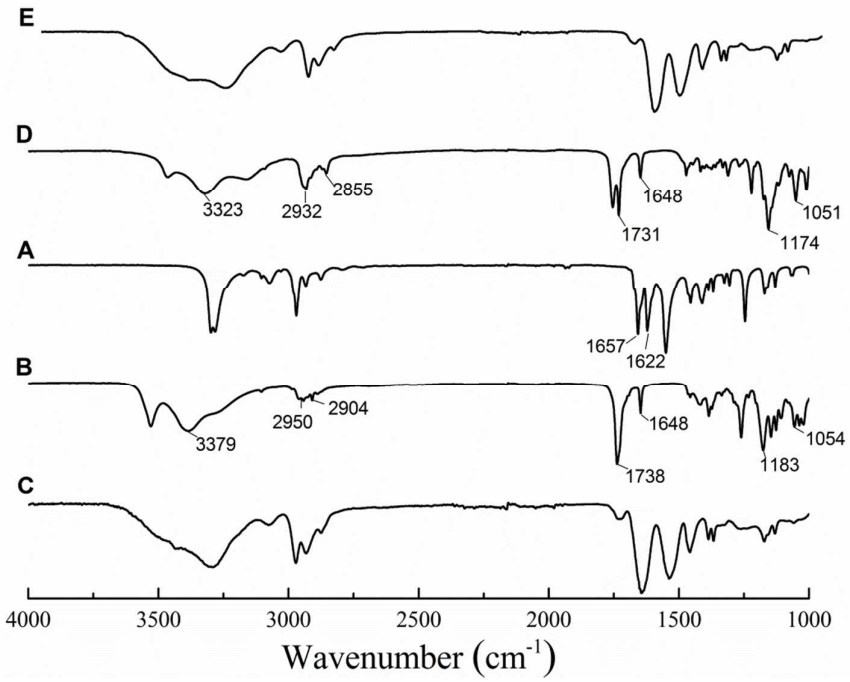

Figure S1. Infrared spectra of (A) PNIPAM; (B) Poly-OVDG; (C) PND-2 (OVDG: NIPAM ratio 1:10); (D) Poly-OVZG; (E) PNZ-1 (OVZG: NIPAM ratio 1:10).